IEEE Access
Multidisciplinary ⋮ Rapid Review ⋮ Open Access Journal

Received March 6, 2022, accepted March 25, 2022, date of publication April 18, 2022, date of current version June 9, 2022.

Digital Object Identifier 10.1109/ACCESS.2022.3168742

Multistage Adaptive Noise Cancellation Scheme for Heart Rate Estimation From PPG Signal Utilizing Mode Based Decomposition of Acceleration Data

MD. TOKY FOYSAL TALUKDAR[1], NAQIB SAD PATHAN[2], SHAIKH ANOWARUL FATTAH[1], (Senior Member, IEEE), MUHAMMAD QUAMRUZZAMAN[2], AND MOHAMMAD SAQUIB[3], (Senior Member, IEEE)

[1]Department of Electrical and Electronic Engineering, Bangladesh University of Engineering and Technology, Dhaka 1000, Bangladesh
[2]Department of Electrical and Electronic Engineering, Chittagong University of Engineering and Technology, Chattogram 4349, Bangladesh
[3]Department of Electrical Engineering, The University of Texas at Dallas, Richardson, TX 75080, USA

Corresponding author: Shaikh Anowarul Fattah (fattah@eee.buet.ac.bd)

ABSTRACT Photoplethysmography (PPG) has recently become a popular method for heart rate estimation due to its simple acquisition technique. However, the main challenge in determining the heart rate from the PPG signals is its high vulnerability to motion artifacts (MA). In this paper, a new scheme is proposed for heart rate estimation through frame selective multistage adaptive noise cancellation (MANC). The frame selective approach determines the specific frames of PPG signal which are significantly interfered with MA, and the MA removal operation is only employed over those specific frames. The MANC scheme is implemented through the Least Mean Square (LMS) algorithm in which instead of the conventional approach of using accelerometer data directly, we propose to utilize mode-based decomposed 3-channel accelerometer data as reference signals independently in a sequential manner. The use of decomposed modes offers high degrees of controllability in the ANC scheme depending on the overlap between the spectra corresponding to MA and heart rate, thereby offers effective denoising. A peak searching algorithm is employed to estimate heart rate-related peaks from the resulting noise-reduced PPG signal. The novelty of the proposed scheme lies in the use of decomposed reference inputs to the MANC algorithm (named as DERMANC scheme) which is accomplished through both empirical mode decomposition (EMD) and variational mode decomposition (VMD). Performance of the proposed EMD and VMD based schemes (E-DERMANC and V-DERMANC) has been tested on a publicly available dataset and very satisfactory results are obtained in terms of estimation accuracy and computational time (0.95 and 1.10 BPM, respectively on 12 recordings) that makes the schemes worthy to be implemented in wearable devices.

INDEX TERMS Acceleration data, adaptive noise cancellation (ANC), empirical mode decomposition (EMD), heart rate, motion artifacts, photoplethysmography (PPG), variational mode decomposition (VMD).

I. INTRODUCTION

In biomedical applications, the measurement of heart rate (HR) is a good way to measure the level of physical fitness. The traditional HR measurement techniques mostly utilize electrocardiogram (ECG) that can measure the HR almost accurately. But its prodigious instrumental setup has recently led to explore many other alternatives to measure HR more conveniently and photoplethysmogram (PPG) is one of them [1]. The periodicity of the PPG signals corresponds to the cardiac rhythm helps to estimate HR using PPG signals simply recorded from the wearers' wrist [2]. The technique is not only flexible but also of significantly low cost. Many wearable devices are available to estimate HR in real-time using PPG signals. However, the main obstacle for these estimators is that the PPG signals are remarkably vulnerable to motion artifacts (MA), which strongly interfere with HR monitoring. Additionally, the shapes of the PPG waveform

The associate editor coordinating the review of this manuscript and approving it for publication was Derek Abbott.

differ from subject to subject and also vary with the location and manner in which the PPG sensor is attached. Hence it is a great challenge to remove MA from the PPG signals, considering the variation of the PPG signals with subjects.

To combat the challenges, many signal processing techniques have already been proposed during recent years to estimate HR accurately from different PPG signals [2]–[20]. A framework called TROIKA proposed a sparse signal reconstruction-based denoising technique where PPG signal is decomposed using singular spectral analysis (SSA) method and then MA-related components are removed using the information from simultaneously recorded acceleration data [2]. Nonetheless, it was computationally intensive. That method is further enhanced in [9], referred to as JOSS, where denoising was performed using a joint sparse spectrum subtraction. Spectral subtraction based denoising algorithms are also used for HR estimation in [8], [10], but the main problem associated here is that it fails to remove noise without deteriorating HR information due to the significant spectral overlapping between MA and HR.

Different denoising schemes based on signal decomposition techniques are also employed in HR estimation. In [21], [22], PPG signal is decomposed using empirical mode decomposition (EMD) and MA-related modes are removed using the noise-related information obtained from the spectrum of accelerometer data. However, it is observed that EMD cannot distinguish very close frequencies [23]. For this reason, an additional recursive least square (RLS) based adaptive noise cancellation (ANC) scheme is also needed in those methods. In another work, recorded PPG signal is viewed as a composition of HR-related information along with the limited number of MA components [24]. Here variational mode decomposition (VMD) is employed in decomposing both the PPG signals and accelerometer data. Next, frequency components dominating in extracted modes from PPG and accelerometer are compared to determine HR-related mode. However, one major drawback to obtain precise HR from the PPG signal, all of the MA components are needed to be distinguished separately. Using decomposition of PPG signal to estimate HR, the distinction is only possible if there exists a certain spectral gap between an MA component and HR frequency. Though the VMD-based method performs better than EMD-based methods in separating frequencies, it has also several constraints which are analyzed and presented rigorously in [25].

Another popular method to denoise the MA-corrupted PPG signals is the Adaptive Noise Cancellation (ANC) algorithm and several schemes based on it were proposed in numerous research works like [3]–[5], [15], [26], [27]. In [3], a two-stage NLMS adaptive filter is proposed, where the reference signal is generated by subtracting the two-channel PPG signals. In [4], a synthetic noise from the MA corrupted PPG signal is generated to use as a reference signal in the LMS filter, and in [5], Kalman filter is used for this purpose. The RLS-based ANC is also combined with the LMS-based ANC in [15], [27] in order to achieve higher accuracy. However, all these schemes are highly sensitive to the selection of noise reference. Most of the reported methods have used the accelerometer data directly as the reference signals to the ANC algorithm. When accelerometer data are used directly as noise reference, the characteristics of different noise-related modes cannot be utilized separately. However, the use of decomposed 3-channel accelerometer data as reference signal to the ANC algorithm may have a potential outcome that needs to be further investigated, and here lies the novelty of this paper.

In this paper, a new algorithm is proposed based on a frame selective multi-stage adaptive noise cancellation scheme (MANC) utilizing decomposed acceleration data as the reference signal applied to the ANC algorithm. Here a noise energy-based frame selection approach is introduced to sort out the noise corrupted frames primarily and then LMS-based MANC is proposed to remove the effect of noise substantially from the selected frames. The main idea here is to utilize the decomposed accelerometer data as noise reference to the MANC algorithm where both EMD and VMD methods are implemented for decomposition separately. A decomposed mode as noise reference allows more degrees of freedom where different MA-related components can be handled separately by varying the step-size and filter order parameters of LMS-based ANC scheme which is not possible using acceleration data directly. Thus PPG can be denoised effectively without deteriorating HR-related information even there exist a high spectral overlap between MA and HR. This denoising process is followed by an innovative peak tracking algorithm that ensures precise HR estimation. The performance of the proposed method is tested and compared to some recent research works on HR estimation.

II. MATERIALS

The proposed method has been tested on the most widely used and publicly available PPG database, reported in [2]. The PPG signals were recorded using two pulse oximeters with identical green LEDs (609nm), along with a 3-axis accelerometer from 12 different subjects of different ages who were running on a treadmill under a controlled situation. During data recording, each subject ran on a treadmill with changing speeds of $1-2$ km/h for 0.5 min, then at $6-8$ km/h for 1 min, $12-15$ km/h for 1 min, then again at $6-8$ km/h for 1 min, $12-15$ km/h for 1 min and at $1-2$ km/h for the last 0.5 min. Moreover, ECG based signal was also recorded from the chest using wet ECG sensors to calculate the ground truth HR for performance measurement of an algorithm. The sampling rate of all these signals was 125 Hz. The ground truth HR has been computed from an 8s time frame. Each time frame has an overlap of 6s with the previous time frame.

III. PROPOSED METHOD

A recorded PPG signal, d(n) during physical exercise contains HR related information along with motion artifacts (MA).

This can be represented as following equation:

$$d(n) = s_c(n) + \tilde{u_c}(n); \quad n = 0, 1, \ldots.., L-1 \qquad (1)$$

which is a composition of the actual HR component along with its half frequency and harmonic frequency components. On the other hand, the characteristic of embedded MA in acquired PPG signal can also be analyzed using simultaneously recorded 3-ch accelerometer data. For a better understanding on the pattern of MA related components within the range of HR, the periodogram of an average of 3-ch acceleration data is computed and then dominant frequencies are extracted from the recorded data of a specific subject (Subject 07). Here a frequency is considered as a dominant one if there exists a spectral peak at that frequency and the spectral magnitude at that position is at least 0.5 in the normalized scale. After that, these extracted dominant frequencies for different 8-second time windows along with actual HR (ground-truth) are depicted in Fig. 1a. It is found that there exist only a few dominant MA frequencies within the range of HR and these dominant MA frequencies are well separable from each other, and maintain a significant spectral gap among them. However, these MA frequencies can also be found in close proximity to actual HR. In order to investigate the variation of dominant frequencies among all subjects, we consider two dominant frequencies corresponding to the top two spectral magnitudes and define them as the most dominant component (MDC) and the second most dominant component (SMDC). In Fig. 1b, the distribution of the MDC and the SMDC extracted from all subjects are illustrated using a Box plot. It is to be noted that the frequency value of the MDC can be lower or higher than that of the SMDC. For example, two DCs are 70 bpm and 140 bpm and 140 bpm has higher spectral magnitude. In this case, 140 and 70 will be considered as the MDC and SMDC, respectively. As a result, in this figure a wide variation is observed in frequency values of the MDC and SMDC. When the selected two dominant frequencies in each case are ordered as per their values as the lower frequency component (LFC) and higher frequency component (HFC), corresponding distribution of LFCs and HFCs are found more compact and shown in Fig. 1c. It can be inferred from the plot that there exists a spectral gap between the LFC and the HFC and hence it is possible to separate these two components in most of the frames. Considering these facts, recorded PPG can be modeled as follows now:

$$d(n) = \sum_{i=1}^{N} s_i(n) + \sum_{i=1}^{M} \bar{u}_i(n) \qquad (2)$$

where $s_i(n)$ denotes a component related to HR and $\bar{u}_i(n)$ denotes a MA related mode. N and M represent the number of dominant modes in PPG and accelerometer data respectively.

In this paper, an algorithm is proposed to reduce the effect of motion artifacts by removing or suppressing MA components present in d[n] in order to get an accurate estimation of HR. The major steps involved in the proposed algorithm are demonstrated in Fig. 2 with the help of a block diagram. An average of 2-channel PPG data along with separate 3-channel accelerometer data are available as input. At first, a frame selection scheme is designed

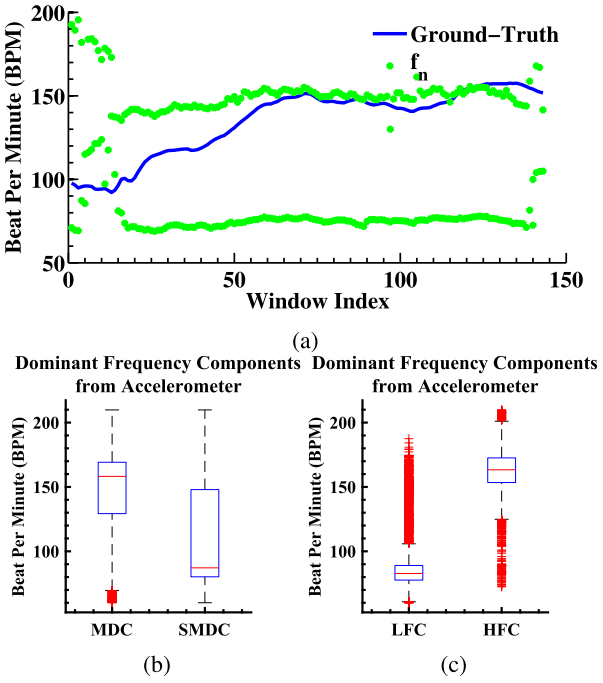

FIGURE 1. a. Dominant frequencies, f_n (denoted by green dots) extracted from accelerometer data are illustrated along with actual heart rate (ground truth) for a single subject (Subject 7). b. Distributions of the most dominant components (MDC) and the second most dominant components (SMDC) are presented in the box plot to visualize the variation among the dominant frequency components in different subjects. c. The distribution of the lower frequency components (LFC) and the higher frequency components (HFC) are depicted which ensures that two separable frequency components exist in most of the accelerometer frames during physical exercise.

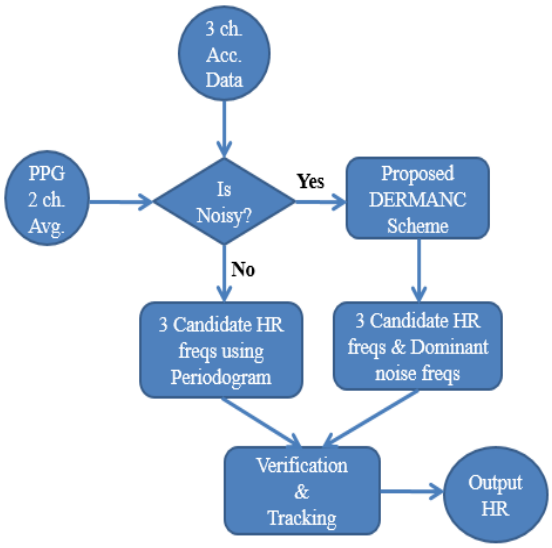

FIGURE 2. Proposed algorithm for HR estimation. Noise corrupted frames are selected and then the proposed DERMANC scheme is employed to estimate the candidate frequencies. Finally, a verification and tracking technique is utilized for the accurate estimation of HR.

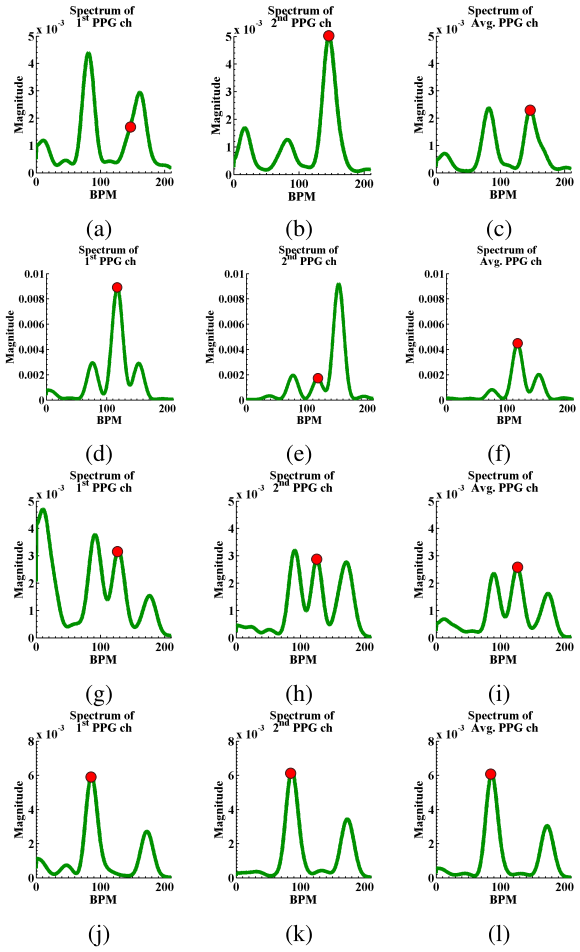

FIGURE 3. Effect of averaging of two channel PPG data shown in spectral domain. Four different cases are considered in four rows depending on the location of original HR (marked by a red circle) on the spectral plot. First row (a-c) corresponds to the *Case I* where 1^{st} channel with a misleading peak and second row (d-f) corresponds to the *Case II* where 2^{nd} channel with a misleading peak. *Case III* (both channels with misleading peak) and *Case IV* (both channels with correct peaks) are depicted in third (g-i) and fourth (j-l) row respectively. The red marker indicates the actual HR (in BPM) for that frame.

to detect the MA-affected frames. Next, the proposed decomposed reference multistage adaptive noise cancellation (DERMANC) scheme is employed over the selected frames to remove the effect of noise substantially. In this scheme, extracted data from each accelerometer channel is decomposed and used as references to the multi-stage adaptive noise cancellation (MANC) blocks. Thereafter, a spectral peak tracking and searching scheme based on prior HR estimates and dominant MA frequencies is introduced to compute the desired HR. Finally, the performance of the proposed method is tested on the most widely used and publicly available PPG database and the results are compared with results obtained by some recent research works on HR estimation.

A. PREPROCESSING

PPG can be measured using a single sensor. However, the dataset used in this work contains pulse oximeter data from two sensors. From the given two-channel PPG data, at first, the average of both channel data is computed instead of using them separately. The averaging operation offers two-fold advantages of utilizing the information contained in both channels and reducing the unwanted random noise. To demonstrate the advantages of using the average of two-channel data in enhancing the desired spectral peak (corresponding to the true HR), spectral representation of PPG data obtained from the 1^{st} channel, the 2^{nd} channel, and the average of the two-channels are shown in Fig. 3 considering four cases from four different subjects.

In *Case I* the spectrum of 1^{st} channel data contains a misleading peak while it shows a better peak in *Case II* for another subject. The opposite result occurs for the 2^{nd} channel data. *Case III* represents the worst condition in which both spectra of 1^{st} and 2^{nd} channels show troublesome peaks to detect HR frequency. *Case IV* shows the best condition in which both channels indicate that HR frequency can easily be computed. But if the average of two-channel data is considered, the HR peak becomes stronger than half frequency peak and second harmonic peak remarkably in all four cases. Thus it is revealed from the pictorial analysis that the averaging of 2 PPG channel data can utilize the HR information properly and reduce the effect of MA in many instances. However, it is not sufficient to eliminate the effect of MA completely from all the PPG frames. Hence, frame selective denoising scheme is employed in proposed algorithm.

B. FRAME SELECTION SCHEME

It is found that the noise energy in the PPG signal is significantly increased during the intense physical exercise stage compared to that at the resting stage. Hence the PPG signal frames are negligibly corrupted by noise at rest conditions, while the effect of noise is prominent in the frames corresponding to intense physical activities. As stated before, the source of this noise is mainly motion artifacts (MA). Most of the conventional methods employ MA removal algorithms on all the PPG signals irrespective of the level of noise. But applying a specific MA removal method, blindly over each signal frame creates a chance of getting degraded HR estimation performance; especially in the frames which are not significantly affected by noise. Here lies the necessity of detecting the frames which are significantly corrupted by noise before employing any noise reduction technique. The effect of MA is to generate unwanted frequencies in the PPG spectrum. With the increase in physical activity, the level of MA increases causing spurious peaks in the PPG spectrum. In view of explaining the fact, two different cases are considered and demonstrated with help of sample cases.

1) CASE I (NOISE FREE PPG SIGNAL)

In Fig. 4, the spectrum of averaged PPG signal along with the spectra corresponding to their 3-channel accelerometer data are depicted where the effect

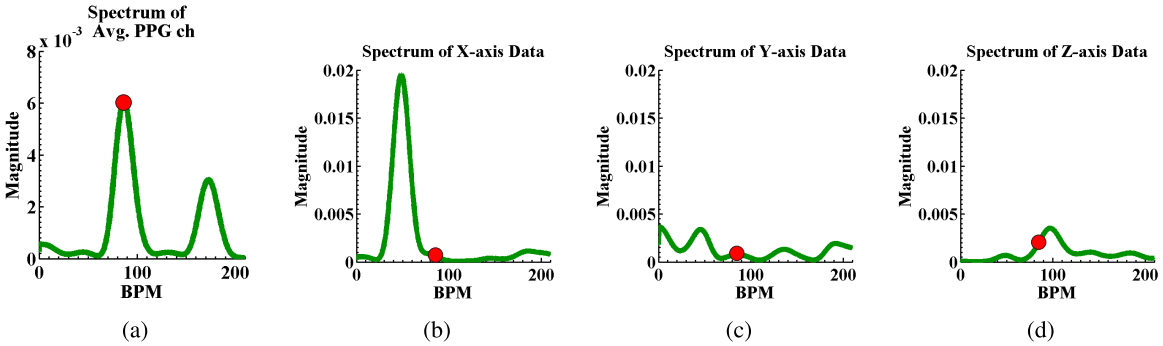

FIGURE 4. Spectrum of the noise free PPG signal (average of two PPG channels) along with acceleration data (X, Y, and Z-axis data) are shown (Case I). The spectrum of the PPG and the accelerometer data are in different scales. The red circle marker indicates the actual HR (in BPM) for that frame. Here it is evident that the effect of MA is not significant in the recorded PPG signal and hence it is possible to estimate HR without any denoising operation.

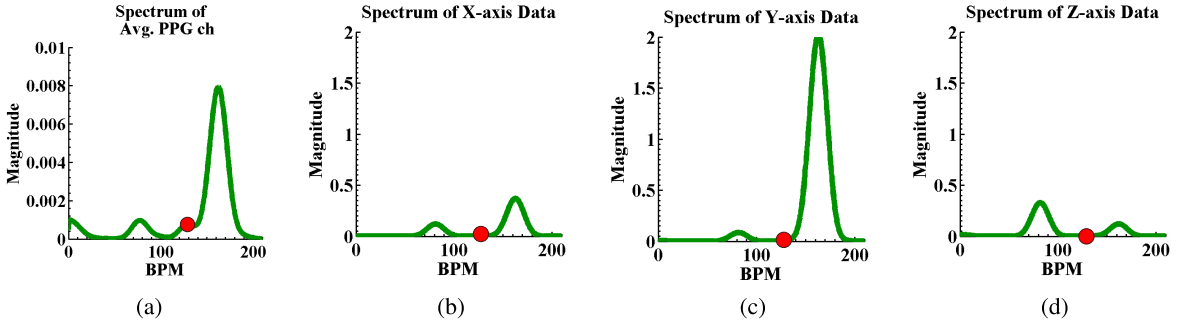

FIGURE 5. Spectrum of the noise corrupted PPG signal (average of two PPG channels) along with acceleration data (X, Y, and Z-axis data) are illustrated (Case II). The spectrum of the PPG and the accelerometer data are in different scales. The red marker indicates the actual HR (in BPM) for that frame. Here the influence of the MA is clearly visible in the spectrum of the PPG signal.

of MA is not significant. On the other hand, the spectrum of a significantly noise-corrupted PPG signal along with the spectra corresponding to their 3-channel accelerometer data are presented in Fig. 5. In case of Fig. 4, in which the PPG spectrum has peaks at its dominant frequency within the range of HR and clearly the true heart rate frequency is located on the most dominant spectral peak of the spectrum. Hence there is no use in employing any MA removal operation over the frames similar to this condition. Even in the case of a weak PPG spectrum, the MA removal operation may degrade the magnitude further, hampering the original HR peak to be detected. Though in the case of a strong PPG spectrum, the MA removal operation will not affect the HR tracking significantly, it is desired to exclude the PPG signal frames from MA removal operation which are not remarkably affected by MA.

2) CASE II (NOISY PPG SIGNAL)

On the contrary, the PPG spectrum shown in Fig. 5 demonstrates the effect of noise in which the energy of accelerometer data is significantly higher compared to that in Fig. 4 (100 times higher shown in the sampled frames). As a result, there is a high chance in this case that the MA noise exhibits significant energy in some frequencies which eventually corrupts the recorded PPG data and may provide false spectral peaks in various locations other than the true HR peaks. Hence a PPG frame, for which the energy of corresponding accelerometer data is very high, needs obvious noise compensation.

In the proposed method, a frame selective approach is introduced which is both computationally and methodically effective to detect the significantly noise-corrupted frames (more specifically MA corrupted frames) first and apply the MA removal operation on those frames only. If a PPG signal frame is found to be corrupted significantly by MA, a noise cancellation scheme is needed to be applied prior to HR estimation from spectral peaks. Otherwise, a peak searching algorithm can be employed directly to estimate HR. In this paper, an energy-based frame selection scheme is proposed to determine the noise corrupted frames. Noise energy of 3 channel acceleration data (for i^{th} frame) is calculated as

$$E_i = \frac{1}{3}\sum_{n=1}^{L}(x_i(n) + y_i(n) + z_i(n))^2 \tag{3}$$

where L is the number of samples in each frame. If this energy exceeds a certain level E_T in a frame, that specific frame is labeled as a noise-corrupted frame and otherwise as a noise-free frame. It is observed that at the beginning and in some cases at other time slots, due to rest condition E_i becomes

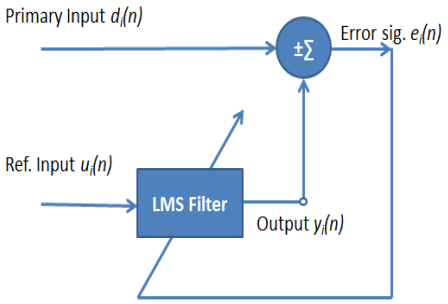

FIGURE 6. Block diagram of an adaptive noise canceller (ANC) scheme. For a input signal $d_i(n)$, the adaptive LMS filter's parameters are updated based on the reference and error signals.

extremely low. Hence finding a suitable threshold value E_T is not a difficult task. For example, it is evident from Fig. 4 that the acceleration data energy representing the noise is significantly low, compared to that of Fig. 5 (100 times lower in the sampled frame). Hence the previous frame is labeled as the noise-free frame, while the next is marked as the noisy-frame in this paper. Thus the noise-energy for each frame is an indicator to determine whether that frame is significantly affected by MA or not. If a frame is found MA-corrupted then denoising is employed over that frame as discussed in the next section.

C. PROPOSED DERMANC SCHEME

From an extensive analysis of the spectral representation of accelerometer data collected with PPG signals, it is found that they contain information related to fundamental hand-swing along with its harmonics, which can be considered as a combination of two or more signals with different spectro-temporal characteristics. Apart from the lead or contact noise, these data represent the MA noise embedded in the recorded PPG signals. The major objective of this paper is to develop a unique scheme for MA removal from the PPG signal and then estimate the HR successfully. Among all the MA removal operations, the adaptive filtering-based noise cancellation methods are getting more popular nowadays considering their real-time applications. Different adaptive filter algorithms are available for the ANC operation. Among them, the least mean squares (LMS) algorithm is a popular, fast, and effective tool due to its low computational burden and ease of implementation. In Fig.6, basic operation of an LMS-based ANC scheme is shown. It is a stochastic gradient algorithm in which it iterates each tap weight of the transversal filter in the direction of the instantaneous gradient of the squared error signal corresponding to the tap weight in question. Performance of ANC scheme using the LMS algorithm depends on step-size parameter, the total number of tap weights, and the most importantly the amplitude of the reference signal [28].

In most of the adaptive filtering algorithms, the noise representing accelerometer data is employed directly as reference

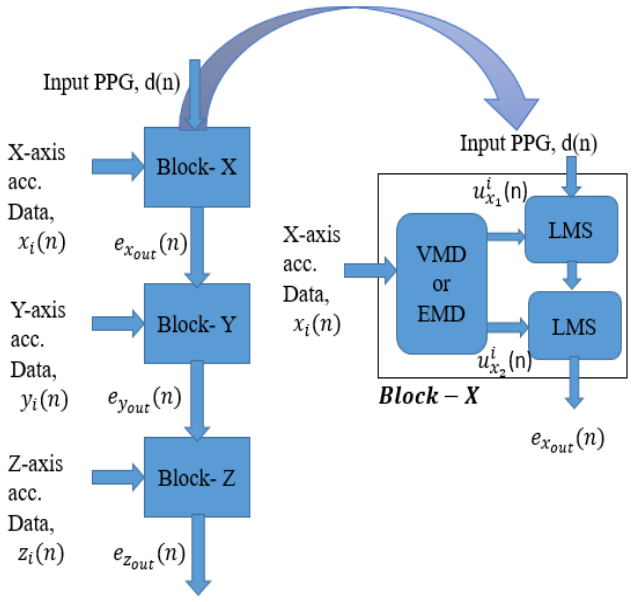

FIGURE 7. Proposed DERMANC scheme. For three channels accelerometer data, we propose 3 separate operating blocks placed serially (ie. Block-X, Block-Y and Block-Z). A sample operation in a block is shown in the right side. Two components obtained by decomposing corresponding acc. data (using EMD or VMD) are used as reference to LMS-based ANC scheme.

signals. As discussed at the beginning of this subsection that the accelerometer data can be better represented as the summation of various component signals. Hence instead of directly using the accelerometer data as reference to the LMS filter, we propose to utilize the component signals as reference. Moreover, we intend to reduce the sensitivity of LMS-based ANC with the variation of the amplitude of the reference signal. For this reason, the accelerometer data are separated through a decomposition technique (EMD or VMD) and then the amplitude of each component signal is normalized to 1. The idea here is to decompose the reference signal into component signals and then by comparing their dominant frequency components with the HR estimates obtained in previous time instances, design a suitable noise compensation strategy. Depending on the separation between the dominant spectral peak of the decomposed signal and the previously estimated HR peak, three levels of noise cancellation are proposed: (i) soft, (ii) moderate, and (iii) hard.

1) Soft denoising: If the dominant frequency of each component is found closely spaced to the previously estimated HR, the task of denoising would be very critical. Here the denoising operation needs to be performed very carefully to reduce the MA related information without affecting the HR information. Although a complete removal of noise may not be possible in this case, the amplitude of the MA related component can be reduced here.
2) Moderate denoising: On the other hand, moderate denoising is employed if a dominant noise frequency appears within a certain range of the previously

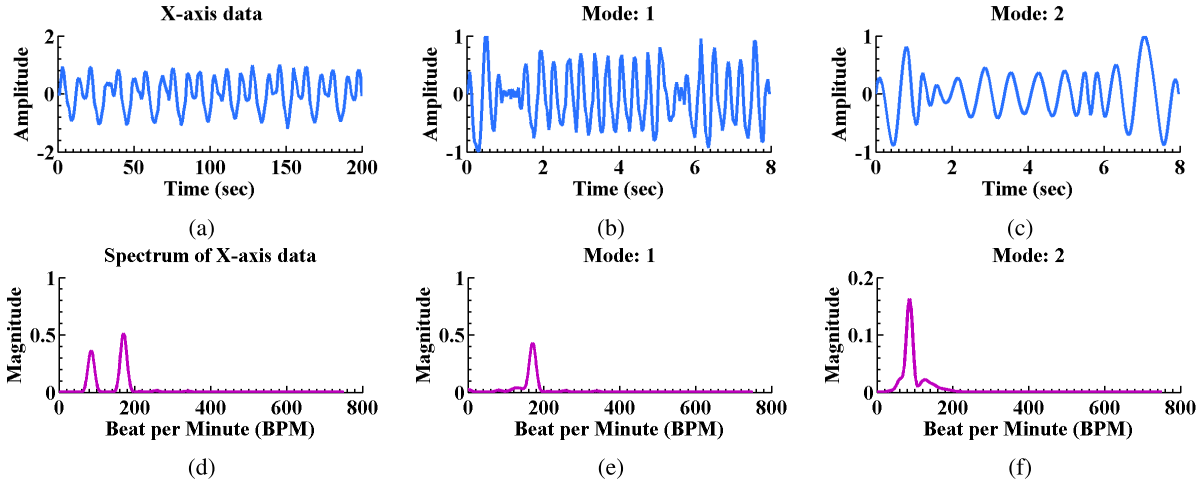

FIGURE 8. Decomposition of a single channel of acceleration data using EMD. Time domain representation of the X-axis accelerometer data, decomposed mode 1, and mode 2, respectively are illustrated through (a)-(c). On the other hand, frequency spectrum corresponding to the X-axis accelerometer data, decomposed mode 1, and mode 2, respectively are depicted (d)-(f).

estimated HR. In this case a relatively stronger denoising is possible but still an attention is required to avoid the information loss.

3) Hard denoising: If there exists a sufficiently large spectral gap between a noise component and the estimated HR in the previous frame, hard denoising is applied to remove that noise component completely from the recorded PPG signal. Here, the possibility of affecting HR related information remains very low when substantial noise removal operation is performed.

The level of denoising operation (i.e. soft, moderate or hard) is controlled by varying the step-size and filter length parameters of the LMS based ANC algorithm. The values of these parameters considered in different scenarios are mentioned in Section IV. In order to understand the impact of different levels of denoising on the HR estimation, let us consider a case where a strong MA component is present very close to the actual HR. In this case, if the ANC is performed just in accordance with the strength of that MA component without considering the spectral proximity with the actual HR, it will certainly deteriorate the necessary HR information. However, in the proposed three-level denoising scheme, here a soft or moderate denoising operation is performed depending on the close spectral proximity, which will ensure the preservation of the necessary HR information. The performances of the single level denoising with different combinations of the parameters and three level denoising will further be presented quantitatively at the graphical analysis part in the *section IV*. The novelty of the proposed method is the utilization of the decomposed accelerometer data as the reference signal for multistage adaptive noise cancellation. Thus all the noise components are expected to be removed or suppressed substantially from the MA-corrupted PPG signals to estimate the desired HR correctly. Due to the use of **DE**composed **R**eference in the **MANC**, the proposed scheme is termed as DERMANC.

For a better understanding, the whole DERMANC algorithm is demonstrated through a block diagram in Fig. 7. At first, the accelerometer data from three channels (x,y,z), labeled as $x_i(n)$, $y_i(n)$ and $z_i(n)$ respectively, are decomposed into several modes which represents the potential noise components $u^i_{x_l}(n)$,$u^i_{y_l}(n)$ and $u^i_{z_l}(n)$, where $l = 1, 2, \ldots\ldots p$, number of modes and i denotes the frame index. Decomposition of accelerometer data using EMD and VMD is depicted in Fig. 8 and Fig. 9, respectively. The prior analysis of noise reveals that the noise signals have only a few dominant peaks within the range of HR frequencies (around 60-180 BPM) and in most of the time number of dominant frequencies is found two, as shown in Fig. 1. Thus the first two modes obtained via VMD or EMD within heart rate range are used for MA removal. In Fig. 7, the candidate PPG signal frame $d(n)$ is used as the signal input to Block-X while the first mode of decomposed X-ch ($x_i(n)$) accelerometer, labeled as $u^i_{x_1}(n)$, is used as the reference input to the first LMS filter. On the right side of Fig. 7, the Block-X is shown in an enlarged view. It can be observed that the input d[n] passes through two LMS blocks where first two modes of proposed decomposed acceleration signal are used as reference sequentially. The output of the first LMS filter of Block-X is then passed to the next LMS filter as input and the second mode of the $x_i(n)$, labeled as $u^i_{x_2}(n)$ as reference input. The output of the Block-X, namely $e_{x_{out}}(n)$ is then fed to Block-Y. Similar to the operations of Block-X, here two filters are used. The successive two stages of LMS filters utilize the two modes $u^i_{y_1}(n)$ and $u^i_{y_2}(n)$ derived from the decomposition operation over Y-axis accelerometer data sequentially as references. Thereafter, output of Block-Y, $e_{y_{out}}(n)$ is passed to Block-Z where the modes $u^i_{z_1}(n)$ and $u^i_{z_2}(n)$ from Z-axis accelerometer data are used as references. It is found at each block that, use of two LMS filters tries to reduce the effect of noise components corresponding to decomposed accelerometer data of a particular channel. As a result, the DERMANC

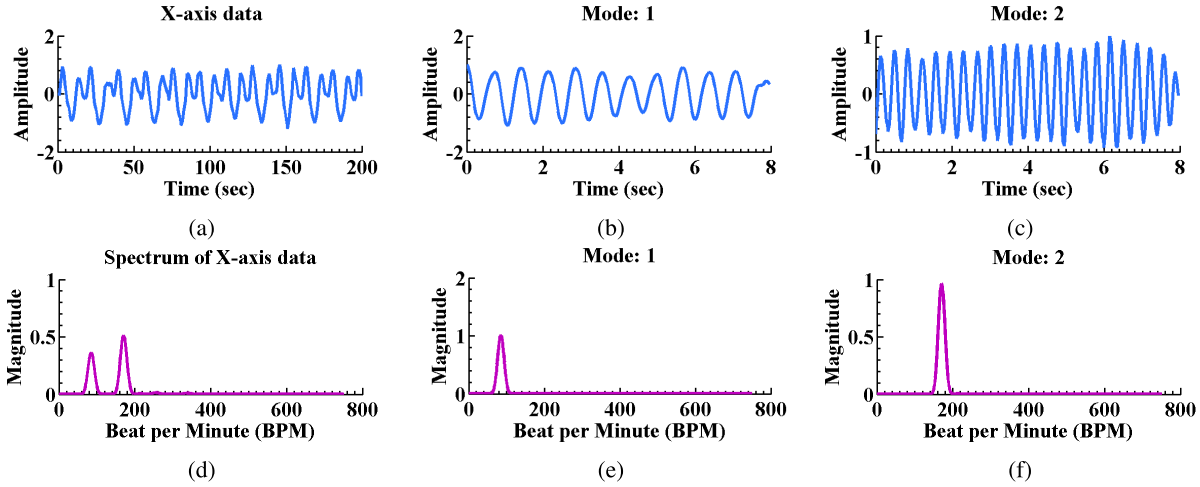

FIGURE 9. Decomposition of a single channel of acceleration data using VMD. Time domain representation of the X-axis accelerometer data, decomposed mode 1, and mode 2, respectively are illustrated through (a)-(c). On the other hand, frequency spectrum corresponding to the X-axis accelerometer data, decomposed mode 1, and mode 2, respectively are depicted (d)-(f).

scheme enhances the performance of the traditional ANC scheme significantly using decomposed mode as reference instead of directly using acceleration data, which has been explored in the *Results and Analysis* section analytically.

D. HEART RATE ESTIMATION THROUGH SPECTRAL PEAK SELECTION SCHEME

For precise HR estimation from noise-reduced PPG signal, Welch's periodogram is deployed. For a sequence $d(n)$ Welch's periodogram is defined as:

$$\hat{D}(e^{j\omega}) = \frac{1}{K \times L \times U} \sum_{i=0}^{K-1} \left| \sum_{n=0}^{L-1} w(n) d(n + im) e^{-jn\omega} \right|^2 \quad (4)$$

Here, $w(n)$ denotes window function, L is the data length of an ensemble, K is the number of ensembles, m represents overlapping factor and U is defined as $U = \frac{1}{L} \sum_{n=0}^{L-1} |w(n)|^2$. From the spectrum obtained through the periodogram, the HR-related peak is expected to be the strongest peak in most cases. However, a noise peak can dominate actual HR in some frames due to the application of soft denoising in those frames as mentioned before. In order to estimate HR accurately in all the situations, initially three candidate peaks (namely f_{pk1}, f_{pk2}, and f_{pk3}) are obtained from the spectrum within the heart rate range (60 to 180 BPM).

These candidate peaks are then verified for the proper estimation of HR using a tracking and verification algorithm. At the beginning of the algorithm, the priority of these three peaks is defined.

- In the case of a noise-free PPG frame, the priority of selected peaks is assigned according to their amplitudes.
- On the other hand, if the frame is detected as noisy, dominant noise frequencies are also obtained from decomposed 3 channel accelerometer data to verify the relevancy of HR estimation.

As mentioned earlier, the proposed DERMANC scheme satisfactorily removes the MA-related modes from recorded PPG signals when the MA-related peaks appear far away from the previous estimation. But in the case of a close MA mode, the ANC scheme is performed in order to suppress MA softly instead of completely eliminating it. Hence, there is the possibility that an MA-related peak may still exist in the denoised PPG signal. In order to overcome this problem, we propose an algorithm where the priority of a peak does not merely depend on its amplitude in the PPG spectrum. Rather priority of different peaks is sorted again when any of the peaks is found close to any MA-related components f_{n_k} where k $= 1, 2, \ldots, 6$. In Algorithm 1, the proposed technique is demonstrated logically.

In Algorithm 1, δf, f_l and f_h are assigned as 2 BPM, 60 BPM and 180 BPM respectively in the proposed method. In the proposed algorithm, the priority of the peaks remain unchanged when the first priority peak is found far from all of the MA-related frequencies. On the contrary, two highest amplitude peaks is shuffled when the first one is close to any of the MA components, while the second one is far. On the other hand, if the first two peaks are found close to any noise frequency, both of their priorities are decreased and the priority of the third highest peak is set to the supreme one. If all of the acquired peaks are found close to any of the MA related frequency, the priority of all peaks are decreased and then there will be no peak with first priority.

After reshuffling, if the first priority peak is found close to the previous HR within a range of Δ_1, it will be considered as current HR. Otherwise, if any of the remaining peaks do not differ more than Δ_2 to the previous HR, then it will be considered as current BPM. Nonetheless, the closer one will be considered as current HR if both of the peaks are found within this range. If none of the above-mentioned conditions is fulfilled, current HR will be considered as the same as the

Algorithm 1: Algorithm for Peak Priority Resolve

```
if (|f_pk1 − f_nk| > δf) && f_l < f_pk1 < f_h then
    f_pk1 ← f_pk1
    f_pk2 ← f_pk2
    f_pk3 ← f_pk3
else
    if (|f_pk2 − f_nk| > δf) && f_l < f_pk2 < f_h then
        tmp ← f_pk1
        f_pk1 ← f_pk2
        f_pk2 ← tmp
        f_pk3 ← f_pk3
    else
        if (|f_pk3 − f_nk| > δf) && f_l < f_pk3 < f_h then
            tmp ← f_pk3
            f_pk3 ← f_pk2
            f_pk2 ← f_pk1
            f_pk1 ← tmp
        else
            f_pk3 ← f_pk2
            f_pk2 ← f_pk1
            f_pk1 ← 0
        end
    end
end
```

last frame. In our performed algorithm, Δ_1 and Δ_2 have been set as 15 BPM and 7 BPM, respectively.

IV. RESULTS AND ANALYSIS

A. PERFORMANCE MEASURES

The evaluation of the performance of our proposed method has been accomplished through five parameters:

1) AAE: The average absolute error (AAE) defined as:

$$\text{AAE} = \frac{1}{\text{W}} \sum_{\text{i}=1}^{\text{W}} |\text{BPM}_{\text{est}}(\text{i}) - \text{BPM}_{\text{true}}(\text{i})| \qquad (5)$$

where W is the total number of time windows.

2) AAEP: The average absolute error percentage (AAEP) is calculated as

$$\text{AAEP} = \frac{1}{\text{W}} \sum_{\text{i}=1}^{\text{W}} \frac{|\text{BPM}_{\text{est}}(\text{i}) - \text{BPM}_{\text{true}}(\text{i})|}{\text{BPM}_{\text{true}}(\text{i})} \qquad (6)$$

3) Band-Altman Plot: The Bland-Altman plot is the third one to examine the agreement between ground-truth and estimates, which shows the difference between each estimate and the associated ground-truth against their average [29].
4) LOA: The Limit of Agreement (LOA), which is defined as: $[\mu - 1.96\sigma, \mu + 1.96\sigma]$, where μ is the average difference and σ is the standard deviation.
5) PCC: The Pearson Correlation Coefficient (PCC) is another parameter to compare the similarities between ground truth and estimated HR values.

B. PARAMETERS SETTING

The frame size used in the proposed method is 8 seconds similar to the ground truth. The noise energy of 3 channel acceleration data(E_i) is utilized in order to distinguish between noisy and noise-free frame. The energy of the accelerometer signal during the exercise is easily distinguishable from the energy found in the rest condition because of very significant differences in these two energy levels. During the rest condition, the energy is found very low and it exhibits very small fluctuations in different frames (over the time). On the contrary, the level of energy is found relatively much higher during the non-rest conditions, for example during physical exercise, walking or running conditions. Although in this case, a wide range of variation is observed in different frames, in each case the energy level is found significantly higher with respect to the rest condition. Hence a threshold value is empirically determined as $E_T = 50$ that offers a sufficient margin between the two classes, rest and non-rest conditions. Different neighboring threshold values are also investigated and no significant differences are observed due to the existence of large separation between the energy levels of the two classes.

The performance of denoising operation based on the LMS algorithm can be controlled by varying the step-size (μ) and filter length (M) parameters. As mentioned earlier, three levels of denoising scheme namely (i) soft, (ii) moderate, and (iii) hard, have been employed in our proposed method. The level of denoising is selected based on the spectral gap between the dominant frequency of an MA component and the previous estimated HR. Soft denoising is employed when that spectral gap is found within 0.083 Hz which is corresponding to 5 BPM. In that case, step-size (μ) is used 0.0004 along with filter length (M) 25. On the other hand, a moderate denoising scheme is employed on the input signal by setting $\mu = 0.0012$ and M=25 when that spectral gap lies between 0.083 Hz and 0.5 Hz. Otherwise, hard denoising is performed using step-size (μ) 0.0012 along with filter length (M) 50.

C. COMPARATIVE ANALYSIS

In this subsection, the performance of the proposed scheme is evaluated in terms of various performance indices. Various conditions are taken into consideration, such as the effect of using the average of the 3 channel accelerometer data directly as the reference signal to the LMS blocks, using these data separately stage by stage, employing EMD for noise decomposition and VMD for the same purpose to use the decomposed signals as reference inputs. The comparative analysis of different cases is described briefly. Moreover, the results of the proposed method are compared with other research works. The tabular and graphical results have been demonstrated analytically.

1) TABULAR ANALYSIS

The performance of the proposed method is demonstrated in two tables. In TABLE 1, AAE and AAEP values obtained for all 12 subjects are reported for both EMD and VMD-based proposed DERMANC schemes. The average AAE for EMD

TABLE 1. AAE and AAEP for all 12 subjects using proposed E-DERMANC and proposed V-DERMANC methods.

Method	Param.	Sub 1	Sub 2	Sub 3	Sub 4	Sub 5	Sub 6	Sub 7	Sub 8	Sub 9	Sub 10	Sub 11	Sub 12	Mean
E-DERMANC	AAE	1.40	1.34	0.60	0.92	0.78	1.28	0.58	0.60	0.45	3.24	1.07	0.97	**1.10**
	AAEP	1.30	1.35	0.48	0.86	0.62	1.08	0.44	0.50	0.38	2.08	0.69	0.68	**0.87**
V-DERMANC	AAE	1.29	1.22	0.64	0.86	0.71	0.87	0.65	0.57	0.44	2.05	1.15	0.98	**0.95**
	AAEP	1.14	1.21	0.54	0.80	0.56	0.70	0.50	0.48	0.37	1.30	0.77	0.70	**0.76**

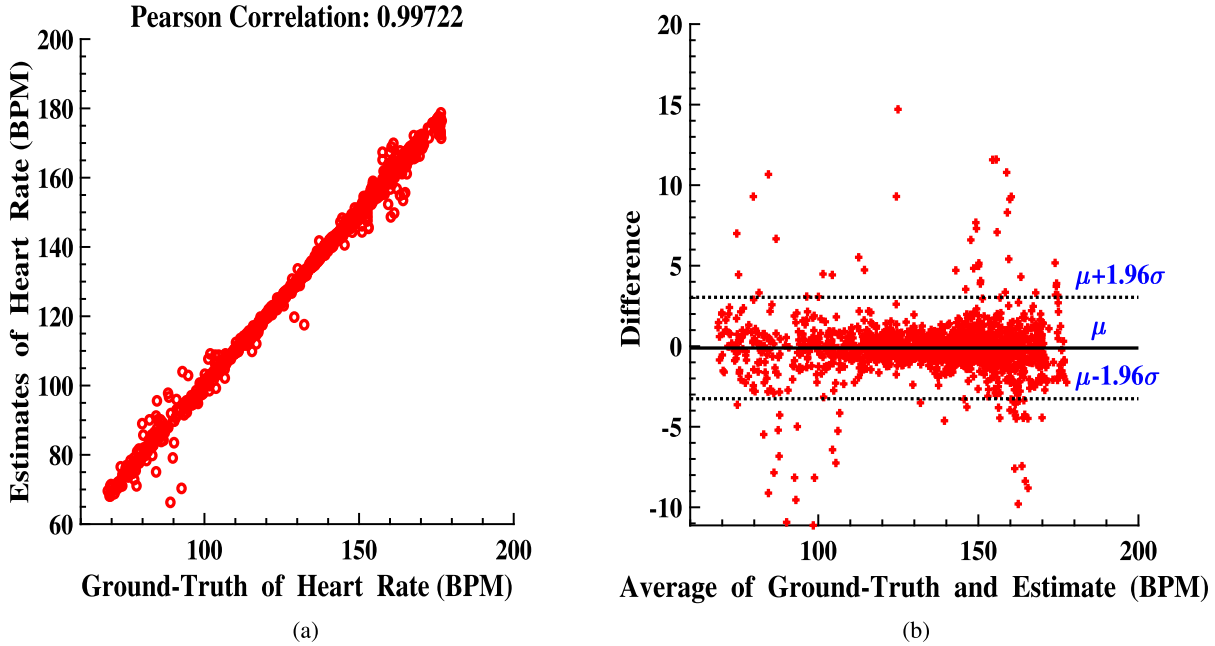

FIGURE 10. (a) Pearson correlation plot between estimated HR and ground truth HR of the estimation on the 12 datasets, (b) Bland-Altman plot showing agreement between ground truth HR and estimated HR on the 12 datasets using V-DERMANC method.

TABLE 2. Comparison among different approaches in terms of performance measures considering all 12 subjects.

Method	AAE	AAEP	LOA	PCC
Case I	2.14	1.63	[-7.43, 8.41]	0.971
Case II	1.38	1.05	[-4.90, 5.23]	0.992
Case III	1.10	0.87	[-4.08, 3.75]	0.994
Case IV	0.95	0.76	[-3.26, 3.04]	0.997
TROIKA [2]	2.14	1.80	[4.79, -7.26]	0.992
JOSS [9]	1.28	1.01	[-5.94, 5.41]	0.993
CPC [15]	1.12	-	[-5.13, 4.87]	0.995
NLMS [26]	1.40	1.16	[-4.71, 4.67]	-
NLMS+RLS [27]	1.03	0.82	-	-

based DERMANC scheme is obtained as 1.10 BPM while it is 0.95 BPM for the VMD-based scheme. Therefore, clearly, the VMD-based proposed DERMANC scheme is depicted as the preferable method.

In Table 2, another analysis is incorporated. The direct use of accelerometer data to the MANC algorithm without decomposition and the decomposed accelerometer data has been reported in this table through four different cases. The four cases are:

Case I (ANC): Using an average of 3-channel accelerometer data as a reference signal to ANC (LMS algorithm).

Case II (MANC): Using 3 channel accelerometer data separately as a reference signal to MANC (LMS algorithm) sequentially.

Case III (E-DERMANC): Using two modes from each of the three accelerometer channels as a reference signal to MANC (LMS algorithm) successively. Here, the modes are extracted using EMD.

Case IV (V-DERMANC): Using two modes from each of the three accelerometer channels as a reference signal to MANC (LMS algorithm) successively. Here, the modes are extracted using VMD.

Simulations are performed in a personal computer with processor Intel Core i5-8265 CPU along with the clock speed of 1.6 GHz. Average computational times required for the HR estimation in the above four cases are found to be **30, 69, 189, and 240** ms, respectively.

It is evident from the tabular analysis that the proposed DERMANC scheme is superior to the method of using an average of 3 channel accelerometer data as a reference signal to the ANC scheme or to the method of using 3 channel accelerometer data separately. Again from *Case III*

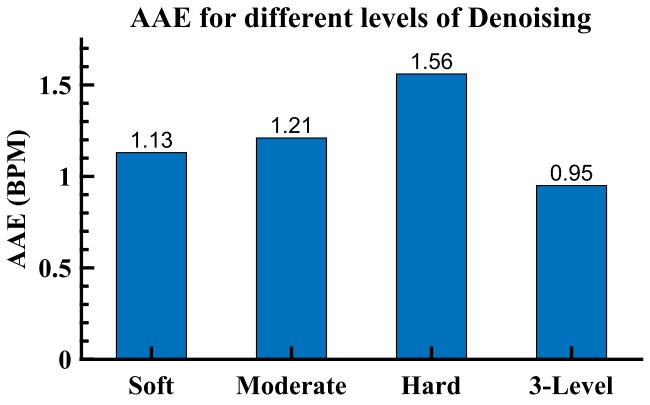

FIGURE 11. The performances of independent soft, moderate or hard denoising schemes are compared with the proposed 3-level denoising scheme in the V-DERMANC algorithm. Here it is evident that the combined scheme offers the best result in terms of average absolute error (AAE).

and *Case IV*, it can be concluded that the VMD-based DERMANC offers better performance although it requires a little bit more time for implementation than the EMD based DERMANC. Furthermore, the performances of the four cases are compared with some state-of-the-art HR estimation methods reported in [2], [9], [15], [26] and [27] in TABLE 2.

To compare with the reported methods in TABLE 2, it can be noted that in the methods of TROIKA [2] and JOSS [9], some initial time windows are excluded by the authors of those papers for performance evaluation. However, in the proposed method (for all four cases), all time windows are taken into consideration. In [15], both LMS and RLS methods are applied to utilize their logical combinations. In [26], Normalized LMS is applied followed by adaptive frequency tracking. Again in [27], the NLMS and RLS-based MANC techniques are applied along with logical combinations which have led to better results. But in each case, the reference signals are applied directly to the ANC scheme without decomposition and here lies the uniqueness of the proposed DERMANC scheme. Case-wise analysis has been explained earlier and case IV i.e. VMD based DERMANC scheme is the best choice among the performed analysis. In brief, it is found that the performance of the proposed method is superior in all subjects in comparison to that obtained by other methods.

2) GRAPHICAL ANALYSIS

In view of investigating the quality of the best choice among the applied methods (V-DERMANC), the estimated HR is plotted against the ground truth considering all time frames of all 12 subjects in Figure 10a. It is observed from the figure that a linear relation exists between the ground truth HR and the estimated HR, and the approximated linear curve passes close to the origin. The Pearson value of the correlation coefficient is found as 0.997, which indicates a very consistent estimation. As it is almost nearly 1, it indicates the validation of a highly accurate estimation of HR.

Next, using all time frames of all 12 subjects Bland-Altman plot is shown in Fig. 10b. It is found that a reasonable limit of agreement (LOA) $[-3.26, 3.04]$ (for the proposed VMD-based DERMANC) is obtained when more than 95% of data exist within 1.96σ. No matter whether the ground truth is very small or large, the difference between estimated values and ground truth is found within a satisfactory limit. Furthermore, the effect of different levels of denoising on the proposed V-DERMANC algorithm is investigated and depicted in Fig. 11. Here, in each case a particular type of denoising (ie. soft, moderate or hard) is applied irrespective of the spectral gap between the MA and estimated HR in the previous frame. The average absolute errors (AAEs) for individual soft, moderate, and hard level of denoising are found to be 1.13 BPM, 1.21 BPM, and 1.56 BPM, respectively. On the other hand, the proposed algorithm with three levels of denoising offers a better solution and can restrict the AAE within 0.95 BPM.

V. LIMITATIONS OF THE STUDY

Similar to the most of the schemes reported earlier, the estimated HR of the previous frame is required to determine the current HR which is a limitation of the proposed method. Although this is a common approach used in different methods, it may cause bias error propagation. Additionally, data used in the proposed scheme are recorded from different subjects using identical devices. For this reason, the robustness of the algorithm for various devices could not be verified here. Furthermore, the data were collected from a group of healthy people within the age range between 18 to 35 which excludes a large portion of the demography.

VI. CONCLUSION

The proposed DERMANC method offers effective denoising of PPG signal by utilizing the modes from decomposed acceleration data as the reference to the MANC scheme, and thus very satisfactory HR estimation is achieved with the use of such denoised PPG signals in a simple spectral estimator. The use of decomposed acceleration data as a reference allows the ANC to deal with a relatively precise target (even when the noise components reside in the close proximity of the HR) and which is found very effective in obtaining better noise reduction in comparison to the case where the reference is used without decomposition. For decomposition, both EMD or VMD are taken into consideration. In each stage of the proposed DERMANC scheme, the ANC needs to handle a single mode instead of more complicated combined signals, which allows a precise ANC operation. Moreover, the use of amplitude normalization along with variable step-size and filter length enhances the controllability of the denoising process in different scenarios.Thus, MA related components are suppressed or removed from PPG signal without deteriorating HR information which was not possible in all frames by using acceleration data directly. Moreover, a unique spectral peak searching scheme based on prior noise estimation and neighbouring HR estimates are also formulated here to compute the desired HR. It is clearly evident from the *Result and Analysis* section that the proposed

VMD based DERMANC scheme is far better than most of the existing methods and it can satisfactorily be used for practical implementation.

ACKNOWLEDGMENT

(Md. Toky Foysal Talukdar and Naqib Sad Pathan contributed equally to this work.)

REFERENCES

[1] J. Allen, "Photoplethysmography and its application in clinical physiological measurement," *Physiolog. Meas.*, vol. 28, no. 3, pp. R1–R39, Mar. 2007.

[2] Z. Zhang, Z. Pi, and B. Liu, "TROIKA: A general framework for heart rate monitoring using wrist-type photoplethysmographic signals during intensive physical exercise," *IEEE Trans. Biomed. Eng.*, vol. 62, no. 2, pp. 522–531, Feb. 2015.

[3] R. Yousefi, M. Nourani, S. Ostadabbas, and I. Panahi, "A motion-tolerant adaptive algorithm for wearable photoplethysmographic biosensors," *IEEE J. Biomed. Health Informat.*, vol. 18, no. 2, pp. 670–681, Mar. 2014.

[4] M. R. Ram, K. V. Madhav, E. H. Krishna, N. R. Komalla, and K. A. Reddy, "A novel approach for motion artifact reduction in PPG signals based on AS-LMS adaptive filter," *IEEE Trans. Instrum. Meas.*, vol. 61, no. 5, pp. 1445–1457, May 2012.

[5] S. Seyedtabaii and L. Seyedtabaii, "Kalman filter based adaptive reduction of motion artifact from photoplethysmographic signal," *Int. J. Electron. Commun. Eng.*, vol. 2, no. 1, pp. 13–16, 2008. [Online]. Available: https://publications.waset.org/vol/13

[6] F. Peng, Z. Zhang, X. Gou, H. Liu, and W. Wang, "Motion artifact removal from photoplethysmographic signals by combining temporally constrained independent component analysis and adaptive filter," *Biomed. Eng. OnLine*, vol. 13, no. 1, pp. 566–568, Dec. 2014.

[7] Q. Wang, P. Yang, and Y. Zhang, "Artifact reduction based on empirical mode decomposition (EMD) in photoplethysmography for pulse rate detection," in *Proc. Annu. Int. Conf. IEEE Eng. Med. Biol.*, Aug. 2010, pp. 959–962.

[8] P.-H. Lai and I. Kim, "Lightweight wrist photoplethysmography for heavy exercise: Motion robust heart rate monitoring algorithm," *IET Healthcare Technol. Lett.*, vol. 2, no. 1, pp. 6–11, 2015. [Online]. Available: https://pubmed.ncbi.nlm.nih.gov/26609397

[9] Z. Zhang, "Photoplethysmography-based heart rate monitoring in physical activities via joint sparse spectrum reconstruction," *IEEE Trans. Biomed. Eng.*, vol. 62, no. 8, pp. 1902–1910, Aug. 2015.

[10] B. Sun and Z. Zhang, "Photoplethysmography-based heart rate monitoring using asymmetric least squares spectrum subtraction and Bayesian decision theory," *IEEE Sensors J.*, vol. 15, no. 12, pp. 7161–7168, Dec. 2015.

[11] Y. Ye, Y. Cheng, W. He, M. Hou, and Z. Zhang, "Combining nonlinear adaptive filtering and signal decomposition for motion artifact removal in wearable photoplethysmography," *IEEE Sensors J.*, vol. 16, no. 19, pp. 7133–7141, Oct. 2016.

[12] M. T. Islam, I. Zabir, S. T. Ahamed, M. T. Yasar, C. Shahnaz, and S. A. Fattah, "A time-frequency domain approach of heart rate estimation from photoplethysmographic (PPG) signal," *Biomed. Signal Process. Control*, vol. 36, pp. 146–154, Jul. 2017. [Online]. Available: https://www.sciencedirect.com/science/article/pii/

[13] Y. Zhang, B. Liu, and Z. Zhang, "Combining ensemble empirical mode decomposition with spectrum subtraction technique for heart rate monitoring using wrist-type photoplethysmography," *Biomed. Signal Process. Control*, vol. 21, pp. 119–125, Aug. 2015. [Online]. Available: https://www.sciencedirect.com/science/article/pii/S1746809415000853

[14] J. Arenas-García, L. A. Azpicueta-Ruiz, M. T. M. Silva, V. H. Nascimento, and A. H. Sayed, "Combinations of adaptive filters: Performance and convergence properties," *IEEE Signal Process. Mag.*, vol. 33, no. 1, pp. 120–140, Jan. 2016.

[15] M. T. Islam, S. T. Ahmed, I. Zabir, C. Shahnaz, and S. A. Fattah, "Cascade and parallel combination (CPC) of adaptive filters for estimating heart rate during intensive physical exercise from photoplethysmographic signal," *Healthcare Technol. Lett.*, vol. 5, no. 1, pp. 18–24, Feb. 2018.

[16] D. Biswas, L. Everson, M. Liu, M. Panwar, B.-E. Verhoef, S. Patki, C. H. Kim, A. Acharyya, C. Van Hoof, M. Konijnenburg, and N. Van Helleputte, "CorNET: Deep learning framework for PPG-based heart rate estimation and biometric identification in ambulant environment," *IEEE Trans. Biomed. Circuits Syst.*, vol. 13, no. 2, pp. 282–291, Apr. 2019.

[17] M. Panwar, A. Gautam, D. Biswas, and A. Acharyya, "PP-Net: A deep learning framework for PPG-based blood pressure and heart rate estimation," *IEEE Sensors J.*, vol. 20, no. 17, pp. 10000–10011, Sep. 2020.

[18] A. Reiss, I. Indlekofer, P. Schmidt, and K. Van Laerhoven, "Deep PPG: Large-scale heart rate estimation with convolutional neural networks," *Sensors*, vol. 19, no. 14, p. 3079, Jul. 2019. [Online]. Available: https://www.mdpi.com/1424-8220/19/14/3079

[19] M. B. Mashhadi, E. Asadi, M. Eskandari, S. Kiani, and F. Marvasti, "Heart rate tracking using wrist-type photoplethysmographic (PPG) signals during physical exercise with simultaneous accelerometry," *IEEE Signal Process. Lett.*, vol. 23, no. 2, pp. 227–231, Feb. 2016.

[20] H. Chung, H. Lee, and J. Lee, "Finite state machine framework for instantaneous heart rate validation using wearable photoplethysmography during intensive exercise," *IEEE J. Biomed. Health Informat.*, vol. 23, no. 4, pp. 1595–1606, Jul. 2019.

[21] E. Khan, F. Al Hossain, S. Z. Uddin, S. K. Alam, and M. K. Hasan, "A robust heart rate monitoring scheme using photoplethysmographic signals corrupted by intense motion artifacts," *IEEE Trans. Biomed. Eng.*, vol. 63, no. 3, pp. 550–562, Mar. 2016.

[22] M. S. Islam, M. Shifat-E-Rabbi, A. M. A. Dobaie, and M. K. Hasan, "PREHEAT: Precision heart rate monitoring from intense motion artifact corrupted PPG signals using constrained RLS and wavelets," *Biomed. Signal Process. Control*, vol. 38, pp. 212–223, Sep. 2017. [Online]. Available: https://www.sciencedirect.com/science/article/pii/S1746809417301015

[23] G. Rilling and P. Flandrin, "One or two frequencies? The empirical mode decomposition answers," *IEEE Trans. Signal Process.*, vol. 56, no. 1, pp. 85–95, Jan. 2008.

[24] W. He, Y. Ye, Y. Li, H. Xu, L. Lu, W. Huang, and M. Sun, "Variational mode decomposition-based heart rate estimation using wrist-type photoplethysmography during physical exercise," in *Proc. 24th Int. Conf. Pattern Recognit. (ICPR)*, Aug. 2018, pp. 3766–3771.

[25] K. Dragomiretskiy and D. Zosso, "Variational mode decomposition," *IEEE Trans. Signal Process.*, vol. 62, no. 3, pp. 531–544, Feb. 2014.

[26] S. Fallet and J.-M. Vesin, "Robust heart rate estimation using wrist-type photoplethysmographic signals during physical exercise: An approach based on adaptive filtering," *Physiolog. Meas.*, vol. 38, no. 2, pp. 155–170, Feb. 2017.

[27] K. R. Arunkumar and M. Bhaskar, "Robust de-noising technique for accurate heart rate estimation using wrist-type PPG signals," *IEEE Sensors J.*, vol. 20, no. 14, pp. 7980–7987, Jul. 2020.

[28] S. Haykin, *Adaptive Filter Theory*. London, U.K.: Pearson, 2008.

[29] J. M. Bland and D. G. Altman, "Comparing methods of measurement: Why plotting difference against standard method is misleading," *Lancet*, vol. 346, no. 8982, pp. 1085–1087, Oct. 1995.

MD. TOKY FOYSAL TALUKDAR received the B.Sc.Engg. degree from the Department of Electrical and Electronic Engineering, Bangladesh University of Engineering and Technology (BUET), Dhaka, Bangladesh, in 2015, where he is currently pursuing the M.Sc.Engg. degree. He stood first in the 37th BCS (Administration) Cadre, in 2018, and currently employed at Bangladesh Civil Service (BCS). His research interests include biomedical signal processing, image processing, nuclear energy, renewable energy, and wireless communication.

NAQIB SAD PATHAN received the B.Sc.Engg. degree in electrical and electronic engineering from the Bangladesh University of Engineering and Technology and the M.Sc.Engg. degree in electrical and electronic engineering from the Chittagong University of Engineering and Technology, Bangladesh. He is currently working as an Assistant Professor with the Department of Electrical and Electronic Engineering (EEE), Chittagong University of Engineering and Technology. His research interests include biomedical image processing, machine learning, VLSI circuit design, and 3D volumetric data processing.

SHAIKH ANOWARUL FATTAH (Senior Member, IEEE) received the B.Sc. and M.Sc. degrees from the Bangladesh University of Engineering and Technology (BUET), Bangladesh, and the Ph.D. degree in electrical and computer engineering (ECE) from Concordia University, Canada. He was a Visiting Postdoctoral at Princeton University, NJ, USA. He is currently a Professor with the Department of Electrical and Electronics Engineering (EEE), BUET. He has published more than 215 international journal articles/conference papers with some best paper awards and delivered more than 80 keynote/invited talks in many countries. His research interests include signal processing, machine learning, and biomedical engineering. He is a fellow of IEB. He is a member of IEEE PES LRP, the IEEE Public Visibility Committee, and the IEEE Smart Village Education Committee. He received several awards, namely the Concordia University's Distinguished Doctoral Dissertation Prize in ENS, in 2009; the 2007 URSI Canadian Young Scientist Award; the Dr. Rashid Gold Medal (in M.Sc. degree); the BAS-TWAS Young Scientists Prize, in 2014; the 2016 IEEE MGA Achievement Award; the 2017 IEEE R10 HTA Outstanding Volunteer Award; and the 2018 IEEE R10 Outstanding Volunteer Award. He served as the Chair/the Founding Chair for different IEEE Society Chapters in Bangladesh, such as IEEE SPS, EMBS, RAS, and SSIT. He was the IEEE Bangladesh Section Chair, from 2015 to 2016. He is the Chair of IEEE PES-HAC. He served on IEEE HAC and various committees for IEEE R10, IEEE EAB, and IEEE SIGHT. He served key positions in many international conferences, such as the General Chair for IEEE R10-HTC2017 and the TPC Chair for IEEE TENSYMP2020. He is an Editorial Board Member of IEEE Access and *BioMed Research International* and an Editor of IEEE PES Enews and *JEE* (IEB).

MUHAMMAD QUAMRUZZAMAN received the B.Sc.Engg., M.Sc.Engg., and Ph.D. degrees from the Department of Electrical and Electronic Engineering, Bangladesh University of Engineering and Technology (BUET), Dhaka, Bangladesh, in 1996, 2002, and 2013, respectively. He has been working as a Faculty Member with the Department of Electrical and Electronic Engineering, Chittagong University of Engineering and Technology (CUET), since 1997, where he is currently a Professor. His research interests include biomedical instrumentation, power electronics, static power converters, and power system protection.

MOHAMMAD SAQUIB (Senior Member, IEEE) received the B.Sc. degree in electrical engineering from the Bangladesh University of Engineering and Technology, Bangladesh, in 1991, and the M.S. and Ph.D. degrees in electrical engineering from Rutgers University, New Brunswick, NJ, USA, in 1995 and 1998, respectively. He worked as a Member of the Technical Staff with the Massachusetts Institute of Technology Lincoln Laboratory; and an Assistant Professor with Louisiana State University, Baton Rouge, LA, USA. He is currently a Professor with the Electrical Engineering Department, The University of Texas at Dallas, Richardson, TX, USA. His current research interests include the various aspects of wireless data transmission, radio resource management, biomedical engineering, and signal processing.